

## Accelerated Publications

---

### Solution Formation of Holliday Junctions in Inverted-Repeat DNA Sequences<sup>†</sup>

Franklin A. Hays,<sup>‡</sup> Virgil Schirf,<sup>§</sup> P. Shing Ho,<sup>\*,‡</sup> and Borries Demeler<sup>\*,§</sup>

*Department of Biochemistry and Biophysics, 2011 Agricultural and Life Sciences, Oregon State University, Corvallis, Oregon 97331-7305, and Department of Biochemistry, MC7760, University of Texas Health Science Center, San Antonio, Texas 78249-3901*

*Received October 18, 2005; Revised Manuscript Received December 22, 2005*

**ABSTRACT:** The structure of Holliday junctions has now been well characterized at the atomic level through single-crystal X-ray diffraction in symmetric (inverted-repeat) DNA sequences. At issue, however, is whether the formation of these four-stranded complexes in solution is truly sequence dependent in the manner proposed or is an artifact of the crystallization process and, therefore, has no relevance to the behavior of this central intermediate in homologous recombination and recombination-dependent cellular processes. Here, we apply analytical ultracentrifugation to demonstrate that the sequence d(CCGGTAC-CCG), which crystallizes in the stacked-X form of the junction, assembles into four-stranded junctions in solution in a manner that is dependent on the DNA and cation concentrations, with an equilibrium established between the junction and duplex forms at 100–200  $\mu$ M DNA duplex. In contrast, the sequence d(CCGCTAGCGG), which has been crystallized as B-DNA, is seen to adopt only the double-helical form at all DNA and salt concentrations that were tested. Thus, the ACC trinucleotide core is now shown to be important for the formation of Holliday junctions in both crystals and in solution and can be estimated to contribute approximately  $-4$  kcal/mol to stabilizing this recombination intermediate in inverted-repeat sequences.

The Holliday junction was proposed more than 40 years ago as a four-stranded intermediate central to homologous recombination (1) and is now recognized as an important component in various cellular mechanisms that expand genomes and maintain their integrity (2). DNA junctions,

as shown from solution studies on immobilized asymmetric constructs (3), come in two flavors: an extended open-X form seen at low salt concentrations and the compact stacked-X form under high-salt conditions (Figure 1). Several single-crystal structures of DNA junctions have been determined since 1999 (4), all from symmetric or near-symmetric inverted-repeat sequences, and generally conform to the model for the stacked-X junction proposed in 1988 (5). One unique feature of the crystal structures is that a specific set of intramolecular interactions within an ACC core trinucleotide have been identified as being important for formation of the junction in the symmetric inverted-repeat sequence motif d(CCnnnN<sub>6</sub>N<sub>7</sub>N<sub>8</sub>GG) (6–8). All substitutions to date within this ACC core are shown to destabilize the junction, resulting in amorphous GCC, ATC, or CCC sequences

---

<sup>†</sup> This work was funded by grants from the National Institutes of Health (R1GM62957A) and the Franco-American Fulbright Commission to P.S.H. and grants from the National Science Foundation (DBI-9974819) and the San Antonio Life Science Institute (SALSI Grant 10001642) to B.D.

<sup>\*</sup> To whom correspondence should be addressed. P.S.H.: telephone, (541) 737-2769; fax, (541) 737-0481; e-mail, hops@onid.orst.edu. B.D.: telephone, (210) 567-6592; fax, (210) 567-6595; e-mail, demeler@biochem.uthscsa.edu.

<sup>‡</sup> Oregon State University.

<sup>§</sup> University of Texas Health Science Center.

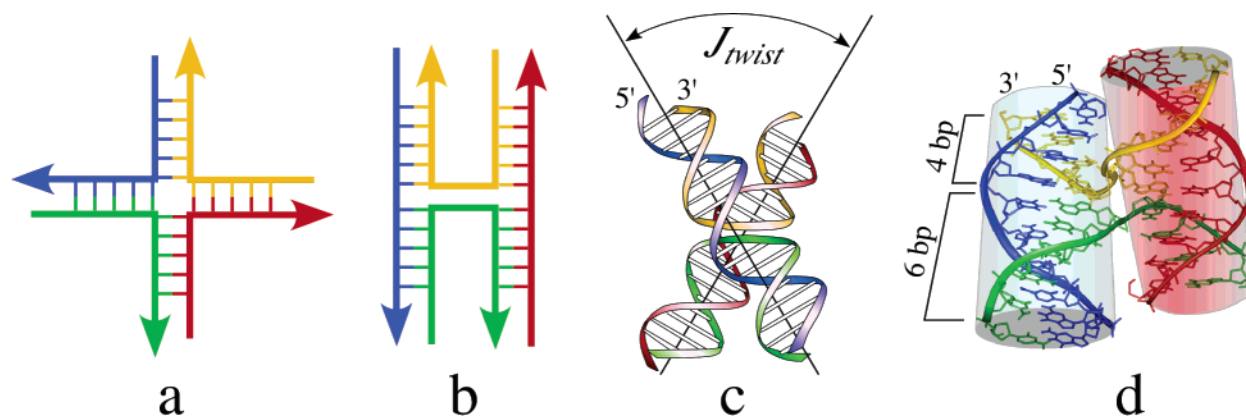


FIGURE 1: Holliday junctions. Schematics of the open-X (a) and stacked-X (b) junctions. (c) Model of the stacked-X junction derived from anomalous gel migration studies of immobilized junctions (5) showing the angle relating the helical axes of the stacked duplex arms [ $J_{\text{twist}}$  (19)]. (d) Single-crystal structure of the inverted-repeat sequence d(CCGGTACCGG) (8), with the 4 bp/6 bp arrangement of stacked arms.

(referring to the unique trinucleotide at  $N_6N_7N_8$ ), which crystallize as both junctions and duplexes, or entirely duplex sequences (as in AGC, which crystallizes as only B-DNA) (6). The implication, therefore, is that Holliday junctions are not free to migrate isoenergetically along symmetric sequences, as is commonly thought, but are fixed by specific sequences. The sequence dependency of branch migration in immobilized symmetric junctions was first demonstrated by Sun et al. (9). Atomic force microscopy and hydroxyl radical footprinting of partially immobilized sequences also showed that the ACC core can direct the geometry and localization of the junction (10). We show here that the same sequence dependency identified in the crystal structures is also true for Holliday junctions formed by the completely symmetric inverted-repeat sequences in solution, with the ACC core conferring significant thermodynamic stabilization to the junction.

## EXPERIMENTAL PROCEDURES

**Synthesis and Purification of Deoxyoligonucleotides.** The DNA sequences 5'-CCGGTACCGG-3' (ACC sequence) and 5'-CCGCTAGCGG-3' (AGC sequence) were purchased from Midland Certified Reagent Co. (Midland, TX) with the 5'-*O*-dimethoxytrityl (DMT)<sup>1</sup> group left attached to facilitate separation from failure sequences and reaction byproducts using preparative reverse-phase HPLC (Microsorb 300 Å pore size C-18 column measuring 250 mm × 21.4 mm at a flow rate of 8 mL/min in 0.1 mM triethylamine acetate with an acetonitrile gradient). The DMT-decanucleotide sequences typically eluted ~31 min postinjection in a mobile-phase concentration of 20% acetonitrile. DMT was removed by treatment with 3% aqueous acetic acid for 15 min with gentle agitation, neutralized with concentrated ammonium hydroxide, and desalted on a Sephadex G-25 (Sigma) column. Purified DNA was stored at -80 °C as a lyophilized powder and redissolved in deionized double-distilled water prior to use, without strand annealing.

**Analytical Ultracentrifugation.** All analytical ultracentrifugation (AUC) experiments were performed at the Center for Analytical Ultracentrifugation of Macromolecular Assemblies at The University of Texas Health Science Center.

Sedimentation experiments were performed using Beckman Optima XL-A and XL-I ultracentrifuges with an An-60Ti rotor. The partial specific volume was estimated to be 0.55 cm<sup>3</sup>/g when sodium is present as the counterion (page 554 of ref 11). Data analyses were performed using UltraScan version 7.1 (<http://www.ultrascan.uthscsa.edu>). Hydrodynamic corrections for buffer conditions were made according to published data (12) and as implemented in UltraScan. Lyophilized DNA samples were suspended in 25 mM sodium cacodylate buffer (pH 7.0), 0.4 mM spermine-4HCl, and corresponding concentrations of CaCl<sub>2</sub> prior to use without strand annealing. DNA concentrations are relative to single-strand populations, except where noted. All sedimentation velocity experiments were performed at 60 000 rpm and 20 °C in aluminum centerpieces. Low-concentration sedimentation velocity experiments using absorption optics measuring at 260 nm were performed in continuous scanning mode (no delays) on 1 OD (~0.01 mM) of the ACC sequence in solutions containing 100, 200, and 400 mM CaCl<sub>2</sub>. These data showed no dependence on salt concentration or junction formation following finite element analysis (13). Higher concentrations (1.02 mM) of the ACC and AGC sequences in 150 mM CaCl<sub>2</sub> and 0.9 mM ACC sequence in 5 mM CaCl<sub>2</sub> were collected using interference optics. Sedimentation coefficients were determined with the enhanced van Holde-Weischet (14) method as implemented in UltraScan. Raw sedimentation velocity data will be provided upon request.

Sedimentation equilibrium experiments were performed at 20 °C with an An-60Ti rotor. All samples were sedimented to equilibrium at 28 500, 36 300, 44 200, 52 100, and 60 000 rpm. These speeds were calculated, on the basis of initial  $\sigma$  values, using the equilibrium speed prediction routine in UltraScan. All equilibrium runs were performed in 25 mM sodium cacodylate (pH 7.0) buffer, 25 mM spermine-4HCl, and 150 mM CaCl<sub>2</sub> with variable initial DNA concentrations as described. Three 110  $\mu$ L samples of the ACC sequence with initial 260 nm absorbance values of 0.3, 0.5, and 0.7 OD were sedimented to equilibrium in a six-sector titanium centerpiece (available from Nanolytics, Gesellschaft für Kolloidanalytik mbH, Berlin, Germany). These samples were prepared using serial dilutions of the 1.02 mM ACC stock solution used in the sedimentation velocity interference experiments described above. The radial step size was 0.001 cm, and each  $c$  versus  $r$  datum point was the average of 20

<sup>1</sup> Abbreviations: AUC, analytical ultracentrifugation; DMT, 5'-*O*-dimethoxytrityl.

independent measurements. Equilibrium was reached when the difference between final scan was minimized. Data points exceeding 0.9 absorbance units were excluded from the analysis. Equilibrium data were initially fit to multiple models; the best fit was to a dimer–tetramer equilibrium model.

**Predicted Sedimentation Coefficients.** Sedimentation coefficients were calculated using HYDROPRO (15) applied to the atomic coordinates of molecular models for the double-helical DNA, and the stacked-X and open-X forms of the DNA junctions (applying 3.1 Å for the bead size, 0.55 cm<sup>3</sup>/g for the partial specific volume, 0.998 g/cm<sup>3</sup> for the solvent density, and 293 K). Coordinates from the single-crystal structure of d(CCGCTAGCGG) (PDB entry 1DCV) were used directly to estimate sedimentation coefficients for the B-DNA duplex. The coefficient for the stacked-X junction was calculated using the atomic coordinates of d(CCGGTACCGG) (8) (characterized by a  $J_{\text{twist}}$  of 40° and two pairs of stacked arms with 4 bp/6 bp arrangements, PDB entry 1DCW). Models of the stacked-X junction with a 60° or 20°  $J_{\text{twist}}$  value were constructed by using the ACC junction and rotating one set of stacked duplex arms 20° or −20°, respectively, about the all-atom junction center and the crystallographic z-axis using XPLOR version 3.851 (16). A model for the 5 bp/5 bp stacked-X junction was generated in XtalView (17) and CNS (18) by attaching a symmetry-related base pair onto the 4 bp junction arms and removing a base pair from each of the 6 bp arms. This structure was then geometry corrected in CNS version 1.1 (18). Coefficients for the open-X junction structure were estimated using the coordinates of the DNA from the Cre–loxP crystal structure (PDB entry 1KBU). The full four-stranded open-X structure was generated in XtalView (17) and then truncated to produce one junction with four arms of equal length (five bases each), and a second junction having two opposing 6 bp arms and two opposing 4 bp arms.

## RESULTS

Sedimentation coefficients ( $S$ ) were determined by analytical ultracentrifugation (AUC) for the inverted-repeat sequence d(CCGGTACCGG), the prototypical stacked-X junction, at various concentrations of DNA and CaCl<sub>2</sub> (Figure 2). At low DNA concentrations, the observed average  $S$  value (1.56  $S$ ) shows the sequence to be a B-DNA double helix [value of 1.55  $S$  predicted for a B-DNA duplex (15)] at all Ca<sup>2+</sup> concentrations. This difference between the predicted and observed  $S$  values may be attributed to either our not taking into account strongly associated cations, the flexibility of the DNA duplex, or both. The sharp edge of the velocity AUC integral distribution plot, however, indicates that the population is homogeneous.

At high DNA and Ca<sup>2+</sup> concentrations (1.02 and 150 mM, respectively), the sedimentation coefficient of the major boundary fraction increases to 2.40  $S$  which is within 2% of the value of 2.44  $S$  calculated (15) from the atomic structure of the d(CCGGTACCGG) stacked-X junction (8) and is significantly higher than the value of 2.2  $S$  expected for the extended open-X form. Thus, we can assert with certainty that this sequence adopts the compact stacked-X form of the Holliday junction in solution under these conditions. We cannot, however, infer any additional information concerning

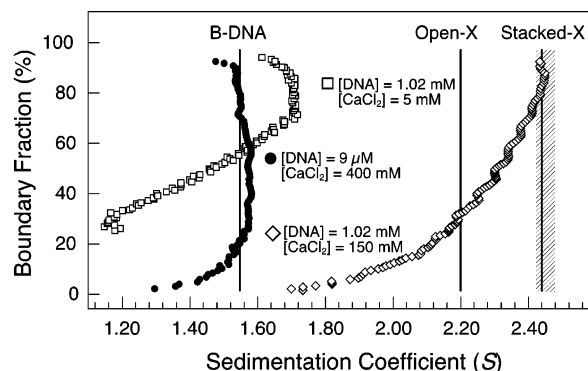


FIGURE 2: Analytical ultracentrifugation integral distribution plots for d(CCGGTACCGG) in 25 mM sodium cacodylate buffer at pH 7.0 and 20 °C, with varied DNA and CaCl<sub>2</sub> concentrations (as labeled). The sedimentation coefficients calculated from the B-DNA structure of d(CCGCTAGCGG) (8), from the DNA coordinates of the open-X junction in the Cre–lox complex (28) (with average 5 bp extended arms), and from the stacked-X junction structure of d(CCGGTACCGG) (8) are labeled. The hashed region indicates the range of coefficients for models of the stacked-X junction with different angles relating the stacked duplex arms (2.44  $S$  for  $J_{\text{twist}}$  = 40°, 2.42  $S$  for  $J_{\text{twist}}$  = 60°, and 2.45  $S$  for  $J_{\text{twist}}$  = 20°, with 4 bp/6 bp stacked arms; see Figure 1d) and with different arrangements of stacked arms (2.44  $S$  for 6 bp/4 bp and 2.48  $S$  for 5 bp/5 bp, and  $J_{\text{twist}}$  = 40°). Differences between the calculated and experimental  $S$  values may reflect systematic errors from the HYDROPRO program not accounting for flexibility in or cation condensation onto the DNA molecules.

the detailed geometry of the junction. The crystal structure of d(CCGGTACCGG) has the four arms of the junction paired such that each semicontinuous duplex arm consists of a 4 bp arm stacked over a 6 bp arm (4 bp/6 bp configuration), and with an angle relating the pairs of stacked arms [ $J_{\text{twist}}$  (19)] of ~40° (Figure 1d). Models constructed for the stacked-X junction with both sharper and more shallow  $J_{\text{twist}}$  angles or with stacking configurations of 5 bp/5 bp or 6 bp/4 bp result in sedimentation coefficients that fall within the range of the expected errors for the observed value. Thus, although the  $S$  value of the major fraction shows excellent agreement with the value predicted from the crystal structure, the AUC results by themselves cannot unequivocally distinguish among structural models with different geometries.

The long tail of the velocity AUC profile indicates that the stacked-X junction is in slow equilibrium with the B-duplex and possibly with the open-X junction. Recent single-molecule studies on the dynamics of DNA junctions implicate the extended open-X structure as an intermediate during junction migration (20). Such a model is consistent with this long tail crossing through the sedimentation profile.

Even at this very high concentration of DNA, the junction dissociates when the calcium concentration is reduced to 5 mM (1.52  $S$ ). In contrast, AUC studies on the sequence d(CCGCTAGCGG), which crystallizes only as B-DNA duplexes (8), show only the double-helical form over all concentration ranges of CaCl<sub>2</sub> and DNA of the current study (data not shown). Thus, DNA junctions in inverted-repeat sequences require high concentrations of both DNA and Ca<sup>2+</sup> and are stabilized specifically by the ACC core in solution as well as in crystals.

An equilibrium constant for dissociation ( $K_D$ ) of the four-stranded junction from B-duplexes (effectively a dimer–



monomer equilibrium relative to duplex DNA) was estimated for the d(CCGGTACCGG) sequence by equilibrium AUC. The observed  $K_D$  of 100–200  $\mu\text{M}$  for the DNA duplex is equivalent to a dissociation free energy ( $\Delta G_D^\circ$ ) of 4.9–5.3 kcal/mol at 20 °C. To translate  $\Delta G_D^\circ$  into a stabilization free energy for the junction ( $\Delta G_j^\circ$ ), we must take into account the dimerization entropy ( $\Delta S_d^\circ$ ) for the equilibrium according to the relationship  $\Delta G_j^\circ = -(\Delta G_D^\circ - T\Delta S_d^\circ)$ . Here,  $\Delta S_d^\circ$  is taken to be  $-5 \pm 4R$  [as estimated by Yu et al. for dimerization of peptides and proteins at a concentration of 1 M in aqueous solution (21)].  $\Delta G_j^\circ$  is thus  $-7.8$  to  $-8.2$  kcal/mol, indicating that each of the two ACC core trinucleotides at the crossover contributes  $-3.9$  to  $-4.1$  kcal/mol to the stabilization of the Holliday junction in solution. This energy is typical for a hydrogen bond (22) and can primarily be attributed to the hydrogen bond from the N4-amino of cytosine at the  $C_8$  position along the sequence to the phosphate oxygen at the junction crossover. This interaction has been identified as being essential in fixing the junction in inverted-repeat sequences, including the prototypical d(CCGGTACCGG) sequence (6).

## DISCUSSION

The sedimentation studies presented here show that DNA Holliday junctions behave in solution in a manner that mirrors that in the crystal system. First, we see that the sedimentation coefficient observed is in excellent agreement (within the error of the measurement) with the value predicted from the atomic structure of the junction in single crystals. This is in stark contrast to other DNA structures, including the G-quartet complexes of the human telomere sequence d(AGGG[TTAGG]<sub>3</sub>), which was seen in the crystal structure to form a parallel G-quartet structure with TTA loops extended in propeller-like fashion (23) but is interpreted to adopt a more compact conformation that is inconsistent with the crystal structure (24). These results for the association of four-stranded junctions indicate that differences in the concentration of DNA must be taken into account when trying to reconcile sedimentation results with crystal structures. For example, if we were to restrict our own studies on junctions to DNA concentrations of 0.25–1.0 OD, the sedimentation results would have indicated that both the ACC and AGC inverted-repeat sequences form only B-DNA duplexes in solution. Which is a better model for the environment of DNA in the cell? The answer to this question could very well be that the higher concentrations used in NMR and crystallization setups more accurately represent the amount of DNA relative to the free volume of the solution in a cellular matrix, as opposed to the dilute solutions studied by optical spectrometric methods.

These studies also demonstrate that there is a strong sequence dependence, as well as concentration dependence, for the formation in solution of the four-stranded DNA junctions. The ACC core trinucleotide of the inverted-repeat sequence motif d(CCGGTACCGG) is shown here to favor formation of the junction in solution as it is in crystals (4, 8), and perturbation of this core (e.g., replacing the  $C_7$  cytosine nucleotide with a guanosine to form the AGC trinucleotide) inhibits formation of the four-stranded complex. Thus, the specific effect of sequence on the formation of Holliday junctions must be considered when trying to understand recombination processes in genomic DNAs. This

is an interesting application of the “indirect readout” concept, where proteins recognize the conformation associated with a particular DNA sequence rather than the sequence itself (25). In this case, a protein would recognize a junction in an inverted-repeat sequence that is stabilized and fixed by the ACC core or, to lesser extents, by the amphimorphic trinucleotides GCC, ATC, and CCC (6).

How often might proteins encounter such stalled junctions in a genome? None of the four junction core trinucleotides are particularly unique, and ACC is in fact about as average as they come (occurring in the human genome approximately as frequently as statistically expected for any random trinucleotide). However, when placed within the context of inverted-repeat sequences, they become highly unique. The occurrence of inverted-repeat sequences  $\geq 8$  bp in length [the terminal base pairs of inverted-repeat decanucleotides are not important determinants in crystallizing junctions (26)] has been estimated at  $\sim 180$  per million bp in eukaryotic genomes (27). Statistically, we would expect only 1 of 455 of such inverted-repeat sequences to include one of the junction core NCC trinucleotides ( $N \neq T$ ), with the NC dinucleotide straddling the point of 2-fold symmetry. This translates to  $\sim 1$  fixed junction per 2.5 million bp (or  $\sim 1400$  sites in the human genome), making them now highly unique and biologically interesting.

## ACKNOWLEDGMENT

We thank Andrea Regier Voth for critically reviewing the manuscript.

## REFERENCES

- Holliday, R. (1964) A mechanism for gene conversion in fungi, *Genet. Res.* 5, 282–304.
- Kuzminov, A. (2001) DNA replication meets genetic exchange: Chromosomal damage and its repair by homologous recombination, *Proc. Natl. Acad. Sci. U.S.A.* 98, 8461–8468.
- Lilley, D. M. J. (2000) Structures of helical junctions in nucleic acids, *Q. Rev. Biochem.* 33, 109–159.
- Hays, F. A., Watson, J., and Ho, P. S. (2003) Caution! DNA crossing: Crystal structures of Holliday junctions, *J. Biol. Chem.* 278, 49663–49666.
- Duckett, D. R., Murchie, A. I. H., Diekmann, S., von Kitzing, E., Kemper, B., and Lilley, D. M. J. (1988) The structure of the Holliday junction, and its resolution, *Cell* 55, 79–89.
- Hays, F. A., Teegarden, A., Jones, Z. J., Harms, M., Raup, D., Watson, J., Cavaliere, E., and Ho, P. S. (2005) How sequence defines structure: A crystallographic map of DNA structure and conformation, *Proc. Natl. Acad. Sci. U.S.A.* 102, 7157–7162.
- Hays, F. A., Vargason, J. M., and Ho, P. S. (2003) Effect of sequence on the conformation of DNA holliday junctions, *Biochemistry* 42, 9586–9597.
- Eichman, B. F., Vargason, J. M., Mooers, B. H. M., and Ho, P. S. (2000) The Holliday junction in an inverted repeat sequence: Sequence effects on the structure of four-way junctions, *Proc. Natl. Acad. Sci. U.S.A.* 97, 3971–3976.
- Sun, W., Mao, C., Liu, F., and Seeman, N. C. (1998) Sequence dependence of branch migratory minima, *J. Mol. Biol.* 282, 59–70.
- Sha, R., Liu, F., and Seeman, N. C. (2002) Atomic force microscopic measurement of the interdomain angle in symmetric Holliday junctions, *Biochemistry* 41, 5950–5955.
- Cantor, C. R., and Schimmel, P. R. (1980) *Biophysical Chemistry*, 2nd ed., Vol. II, W. H. Freeman and Company, New York.
- Laue, T. M., Shah, B. D., Ridgeway, T. M., and Pelletier, S. L. (1992) Computer-aided interpretation of analytical sedimentation data for proteins, in *Analytical ultracentrifugation in biochemistry*

- and polymer science (Harding, S. E., Rowe, A. J., and Horton, J. C., Eds.) pp 90–125, Royal Society of Chemistry, Cambridge, U.K.
13. Demeler, B., and Saber, H. (1998) Determination of molecular parameters by fitting sedimentation data to finite-element solutions of the Lamm equation, *Biophys. J.* **74**, 444–454.
  14. Demeler, B., and van Holde, K. E. (2004) Sedimentation velocity analysis of highly heterogeneous systems, *Anal. Biochem.* **335**, 279–288.
  15. Garcia De La Torre, J., Huertas, M. L., and Carrasco, B. (2000) Calculation of hydrodynamic properties of globular proteins from their atomic-level structure, *Biophys. J.* **78**, 719–730.
  16. Brünger, A. T. (1992) *X-PLOR version 3.1: A system for X-ray crystallography and NMR*, Yale University Press, New Haven, CT.
  17. McRee, D. E. (1999) XtalView/Xfit: A versatile program for manipulating atomic coordinates and electron density, *J. Struct. Biol.* **125**, 156–165.
  18. Brünger, A. T., Adams, P. D., Clore, G. M., DeLano, W. L., Gros, P., Grosse-Kunstleve, R. W., Jiang, J. S., Kuszewski, J., Nilges, M., Pannu, N. S., Read, R. J., Rice, L. M., Simonson, T., and Warren, G. L. (1998) Crystallography & NMR system: A new software suite for macromolecular structure determination, *Acta Crystallogr. D54* (Part 5), 905–921.
  19. Watson, J., Hays, F. A., and Ho, P. S. (2004) Definitions and analysis of DNA Holliday junction geometry, *Nucleic Acids Res.* **32**, 3017–3027.
  20. McKinney, S. A., Declais, A. C., Lilley, D. M., and Ha, T. (2003) Structural dynamics of individual Holliday junctions, *Nat. Struct. Biol.* **10**, 93–97.
  21. Yu, Y. B., Privalov, P. L., and Hodges, R. S. (2001) Contribution of translational and rotational motions to molecular association in aqueous solution, *Biophys. J.* **81**, 1632–1642.
  22. Perrin, C. L., and Nielson, J. B. (1997) “Strong” hydrogen bonds in chemistry and biology, *Annu. Rev. Phys. Chem.* **48**, 511–544.
  23. Parkinson, G. N., Lee, M. P., and Neidle, S. (2002) Crystal structure of parallel quadruplexes from human telomeric DNA, *Nature* **417**, 876–880.
  24. Li, J., Correia, J. J., Wang, L., Trent, J. O., and Chaires, J. B. (2005) Not so crystal clear: The structure of the human telomere G-quadruplex in solution differs from that present in a crystal, *Nucleic Acids Res.* **33**, 4649–4659.
  25. Otwinowski, Z., Schevitz, R. W., Zhang, R. G., Lawson, C. L., Joachimiak, A., Marmorstein, R. Q., Luisi, B. F., and Sigler, P. B. (1988) Crystal structure of trp repressor/operator complex at atomic resolution, *Nature* **335**, 321–329.
  26. Thorpe, J. H., Gale, B. C., Teixeira, S. C., and Cardin, C. J. (2003) Conformational and Hydration Effects of Site-selective Sodium, Calcium and Strontium Ion Binding to the DNA Holliday Junction Structure d(TCGGTACCGA)<sub>4</sub>, *J. Mol. Biol.* **327**, 97–109.
  27. Schroth, G. P., and Ho, P. S. (1995) Occurrence of potential cruciform and H-DNA forming sequences in genomic DNA, *Nucleic Acids Res.* **23**, 1977–1983.
  28. Gopaul, D. N., Guo, F., and Van Duyne, G. D. (1998) Structure of the Holliday junction intermediate in Cre-loxP site-specific recombination, *EMBO J.* **17**, 4175–4187.

BI052129X